Energy and Power Engineering, 2015, 7, 258-269
Published Online June 2015 in SciRes. http://www.scirp.org/journal/epe
http://dx.doi.org/10.4236/epe.2015.76025

Impact of the Fermeuse Wind Farm on Newfoundland Grid

Seyedali Meghdadi, Tariq Iqbal

Department of Electrical Engineering, Memorial University of Newfoundland, St. John's, Canada
Email: s.meghdadi@mun.ca, tariq@mun.ca

Received 10 March 2015; accepted 15 June 2015; published 18 June 2015

Abstract

This paper aims to study the impact of the Fermeuse wind farm (46˚58'42"N 52˚57'18"W) through simulation of wind turbines driven by doubly fed induction generator which feed AC power to the isolated utility grid of Newfoundland. The focus is on the determination of both voltage and system stability constraints. The complete system is modeled and simulated in Matlab Simulink environment.

Keywords

Renewable Energy Systems, Fermeuse Wind Farm, Wind Turbine, Doubly Fed Induction Generator, Wind Energy Conversion Systems

1. Introduction

Every day decreases in the cost of renewable energy generators, increasing demand for renewable energy sources to provide a sustainable future, and worldwide regulations to reduce greenhouse gas emissions have made renewable energy sources become the strongest candidates to substitute for oil/gas power plants. The demand for more power combined with interest in clean technologies has driven researchers to develop distributed power generation units using renewable energy sources [1]-[2]. The employment of these distributed generations in power systems can offer benefits as follows:

- Reliable Power Supply:

Any unexpected events, such as grid faults occurring in the upstream power lines, result in a disconnection of the distributed generation unit from the grid, causing black-outs. However, in this situation, the autonomous operation of a group of distributed generation units can provide power to local loads.

- Power Loss Compensator:

Many rural communities in Canada are generally connected to the central power stations through long trans-

How to cite this paper: Meghdadi, S. and Iqbal, T. (2015) Impact of the Fermeuse Wind Farm on Newfoundland Grid. *Energy and Power Engineering*, **7**, 258-269. http://dx.doi.org/10.4236/epe.2015.76025

mission lines or obtain their power supply through diesel generators. Delivering power to those communities from a central power station causes a significant amount of loss. In Newfoundland, the power loss in the transmission system is about 9% [3]. Therefore, the formation of small renewable energy plants around these rural areas can significantly reduce the amount of power.

- Reduction in Transmission System Expansion:

According to the Newfoundland and Labrador Hydro's (NLH) 2010 long term planning load forecast, power demand is predicted to grow at 1.3 percent per year through 2029. This increase requires more power transmission infrastructure, which may not be economically feasible because of the higher cost involved in new transmission lines installation and maintenance for rural areas. Therefore, the installation of renewable plants near the user load eliminates the requirement of re-designing new long transmission lines, resulting in cost savings.

This paper presents a dynamic model of a 27 MW wind farm located in Fermeuse, Newfoundland, Canada. The wind farm system model is simulated in Matlab/Simulink with the purpose of investigating the effects of wind speed variations on voltage and frequency of the grid.

2. System Components

2.1. Wind Power Generation System

The Fermeuse wind farm model consists of 9 dynamic models of variable-speed, doubly-fed induction generator based wind energy conversion systems (WECS). Each variable speed, doubly-fed induction generator contains the model of a variable pitch wind turbine rotor and a wound rotor asynchronous generator. The rotor winding is connected to the grid using a back-to-back pulse width modulated (PWM) voltage source converter (GEC and SEC), where the stator is directly connected to the grid. The Vestas-90 WECS is utilized in the proposed system, with the topology shown in **Figure 1**. The decouple control technique is incorporated to control the converters in the rotor side [4].

2.2. Wind Turbine

In steady state, the mathematical power developed by the wind turbine P_m, can be expressed by the following set of equations:

$$P_m = C_p(\lambda,\beta)\frac{\rho A}{2}\upsilon^3$$

$$C_p(\lambda,\beta) = C_1\left(\frac{C_2}{\lambda_i} - C_3\beta - C_4\right)e^{\frac{-C_5}{\lambda_i}} + C_6\lambda$$

$$\frac{1}{\lambda_i} = \frac{1}{\lambda + C_7\beta} - \frac{C_8}{\beta^3 + 1}$$

$$\lambda = \frac{R\omega}{\upsilon}$$

Mechanical torque T_m, is the ratio of mechanical power to turbine speed.

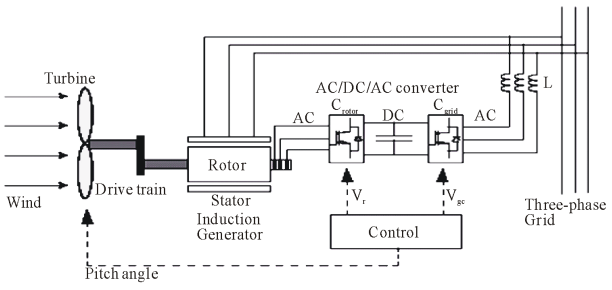

Figure 1. Schematic of a variable speed doubly-fed induction generator based wind energy conversion system.

$$T_m = \frac{P_m}{\omega}$$

where $C_p(\lambda, \beta)$, A, υ, and β are power coefficient, sweep area, wind speed ,and pitch angle respectively.

2.3. Two-Mass Model of Drivetrain

In [5] it is indicated that the three-mass model can be reduced to a two-mass model by considering an equivalent system with an equivalent stiffness and damping factor. The moment of inertia for the shafts and the gearbox wheels can be neglected because they are small compared with the moment of inertia of the wind turbine or generator. Therefore the resultant model is essentially a two mass model connected by a flexible shaft. Only the gearbox ratio has influence on the new equivalent system.

The dynamic equations can be written in two points: the wind turbine side with the influence of generator component through the gearbox and on the generator side respectively. The equivalent system on the generator side is shown in **Figure 2**.

The dynamic equations of the drive-train written on the generator side are:

$$T'_{wtr} = J'_{wtr}\frac{\mathrm{d}\Omega''_{wtr}}{\mathrm{d}t} + D'_e\left(\Omega'_{wtr} - \Omega''_{gen}\right) + K'_{se}\left(\theta'_{wtr} - \theta_{gen}\right)$$

$$\frac{\mathrm{d}\theta'_{wtr}}{\mathrm{d}t} = \Omega'_{wtr}$$

$$-T'_{gen} = J_{gen}\frac{\mathrm{d}\Omega_{gen}}{\mathrm{d}t} + D'_e\left(\Omega_{gene} - \Omega'_{wtr}\right) + K'_{se}\left(\theta_{gen} - \theta'_{wtr}\right)$$

$$\frac{\mathrm{d}\theta_{gen}}{\mathrm{d}t} = \Omega_{gen}$$

where T'_{wtr}, J'_{wtr}, Ω'_{wtr}, D'_e, and K'_{se} respectively are wind turbine torque, wind turbine, moment of inertia, wind turbine mechanical speed, damping constant, and spring constant. The equivalent stiffness K'_{se} is given by:

$$\frac{1}{K'_{se}} = \frac{1}{\frac{K_{wtr}}{K^2_{gear}}} + \frac{1}{K_{gen}}$$

And the equivalent moment of inertia for the rotor is:

$$J'_{wtr} = \frac{1}{K^2_{gear}} \cdot J_{wtr}$$

2.4. Generator

The dynamic equivalent (d-q) circuit of a doubly-fed induction machine in a synchronously rotating reference frame is represented in **Figure 2**. Using d-q axis transformation in the synchronously rotating reference frame, the output voltages for the doubly-fed induction generator are implemented based on **Figure 3** [6].

2.5. Converter

The rotor side of the doubly-fed induction generator based wind generator system is connected to the grid through a back-to-back PWM voltage source converter (**Figure 4**). In order to eliminate fluctuations in current, and so output power of wind farm caused by triggering converter, the average model of wind turbine detailed in [7] is used. This model exploits an AC/DC/AC IGBT-based PWM converter modeled by voltage sources. The stator winding is connected directly to the 60 Hz grid while the rotor is fed at variable frequency through the AC/DC/AC converter. The DFIG technology allows extracting maximum energy from the wind for low wind

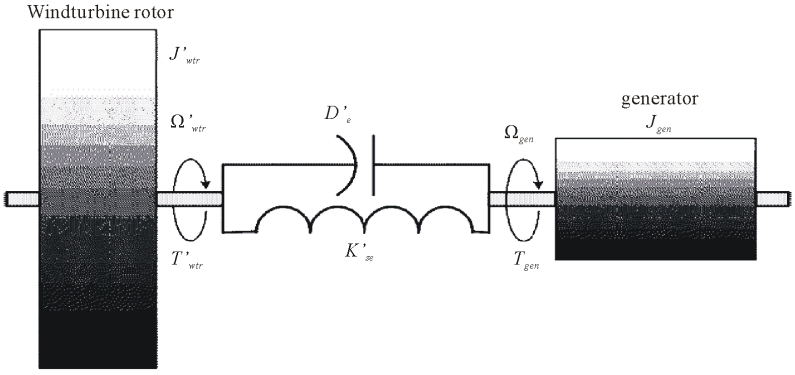

Figure 2. Equivalent diagram of the wind turbine drive train on the generator side.

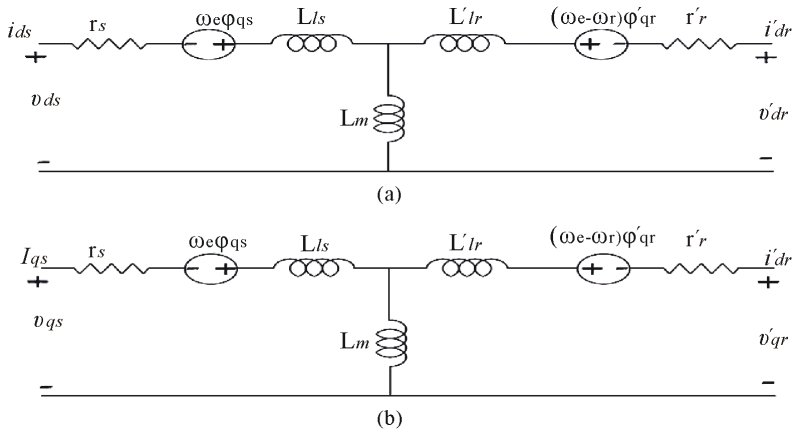

Figure 3. Equivalent circuit representation of an induction machine in synchronously rotating referenced frame: (a) d-axis, (b) q-axis.

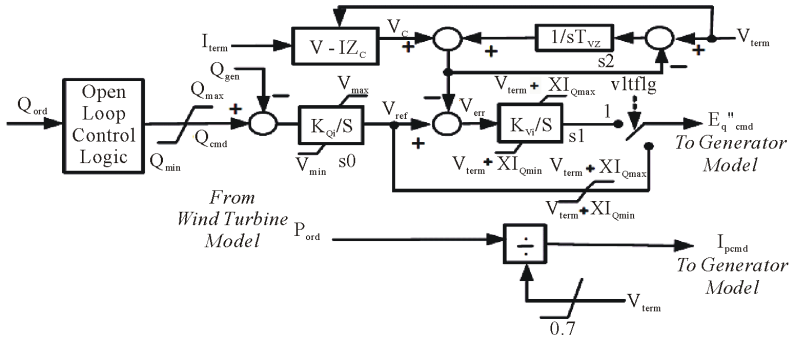

Figure 4. Electrical Control model.

speeds by optimizing the turbine speed, while minimizing mechanical stresses on the turbine during gusts of wind. **Figure 3** depicts the control diagram used in the referenced model [7] [8]. Based on inputs from the turbine model (P_{ord}) and from the supervisory VAR controller (Q_{ord}), the Excitation Control Model dictates the active and reactive power to be delivered to the system.

3. Location of the Wind Farm

Fermeuse is a small rural community located on the southern shore of the Avalon Peninsula on Newfoundland Island in the province of Newfoundland and Labrador, Canada (**Figure 5**).

Figure 5. Bird-eye view of a part of the wind farm.

4. Power System Planning and Operation Criteria

Connection of a wind farm to the grid has a large impact on grid stability. The increased penetration of wind energy into the power system over the last decade has therefore led to serious concern about its influence on the dynamic behavior of the power system. An overview of the national grid requirements in several countries is provided in [9] and main attention is drawn to fault ride-through (*i.e.* requirements imposed to avoid significant loss of wind turbine production in the event of faults) and power control capability (*i.e.* regulating active and reactive power) and performing frequency and voltage control on grid [9].

4.1. Voltage Criteria

Under normal conditions the transmission system is operated such that the voltage is maintained between 95% and 105% of nominal. During contingency events the transmission system voltage is permitted to vary between 90% and 110% of nominal prior to operator intervention. Following an event, operators will take steps (*i.e.* re-dispatch generation, switch equipment in or out of service, curtail load or protection) to return the transmission system voltage to the 95% to 105% normal operating range.

4.2. Stability Criteria

The frequency of a power system can be considered as a measure of the balance or imbalance between production and consumption in the power system. With nominal frequency, production and consumption including losses in transmission and distribution are in balance. If the frequency is below nominal, the consumption of electric energy is higher than production and if it is above nominal the consumption is lower than production [10]. Control of frequency on the island system is the responsibility of NLH's generating stations. Adding non-dispatchable generation to the island may result in fewer on NLH's dispatchable generation resources being on line. As fewer generators are left to control system frequency, frequency excursions become magnified for the same change in load. A theoretical point can be reached where the slightest increase in load will cause the system to become unstable.

5. Single Line Diagram of the System

The nine WTs together are placed in the Fermeuse wind farm block in **Figure 6**. Each of the WTs in the wind farm is a 3 MW variable-speed doubly-fed induction generator wind turbine. The distance between each wind turbine generator is small and neglected. Each wind turbine generator is connected to the line through a transformer, TW, and a short transmission line. The transmission line (TL3) of the wind farm is connected to bus 4, which is eventually connected to bus 2 using a power transformer, T1 (**Figure 7**). Data for the buses of the proposed system are provided in **Table 1**.

Moreover, the data for transmission lines and transformers are provided in **Table 2**.

Figure 6. View of the wind farm from its transformation station.

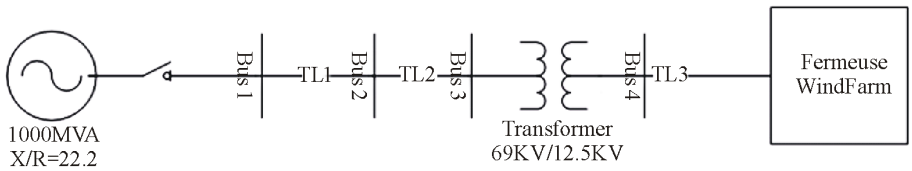

Figure 7. Fermeuse grid connection single line diagram.

Table 1. Fermeuse buses.

BUS	P [MW]	Q [MVAR]	V [KV]
1	ΔP	ΔQ	69
2	ΔP	ΔQ	69
3	0	0	69
4	27	12	12.5

Table 2. Fermeuse transmission Lines and Transformers.

Component	V [KV]	Z [Ω]	S [MVA]
TL1	69	0.002 + j0.0032	40
TL2	69	0.0416 + j0.0663	40
TL3	12.5	0.0374 + j0.3741	40
T1	69/12.5	0.05 + j0.5	40
TW	12.5/1	0.006 + j0.0625	5

6. Simulink Model

The Simulink model is a mathematical interpretation of the explained single line diagram of the system (**Figure 8**). This includes model of wind turbine, transformers, Pi model of transmission lines, utility grid and some measurement blocks. These blocks are connected together to build the model of the system. In the end, injected current and voltage form the wind farm delivered by TL1 to the grid are measured and the output power of the wind farm is calculated through ten seconds of running the simulation.

In order to accurately model wind turbines, data in **Table 3** and **Table 4** were used based on [11].

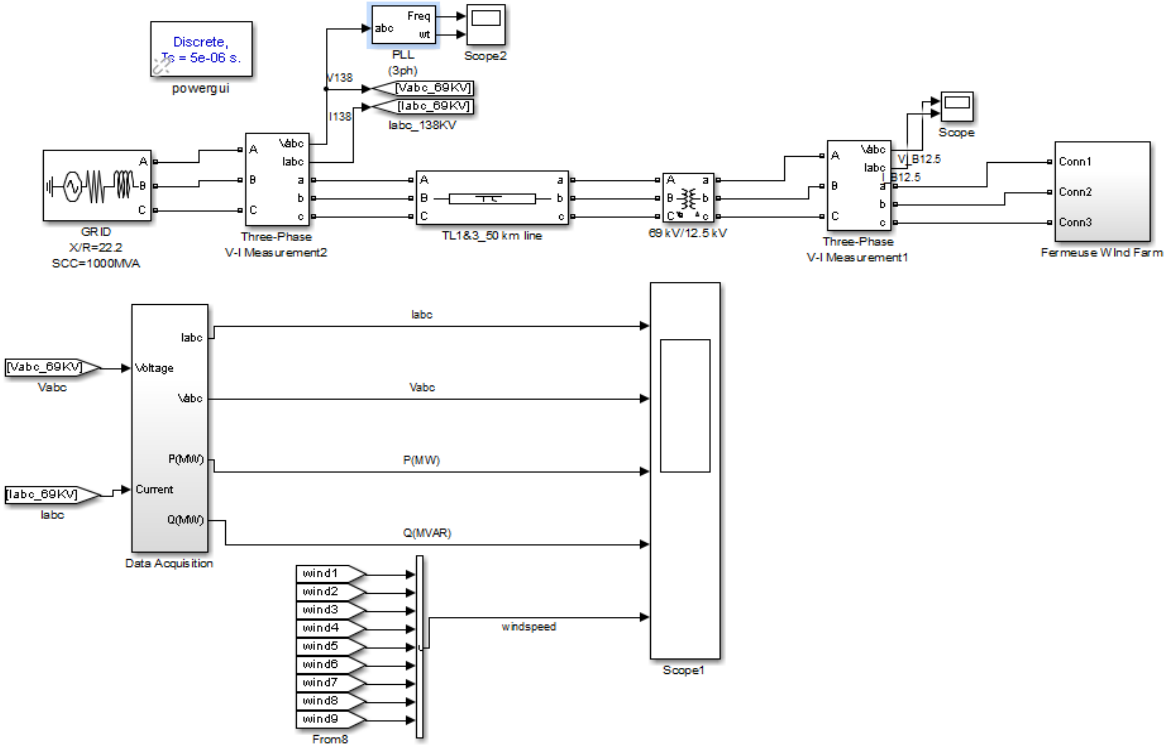

(a)

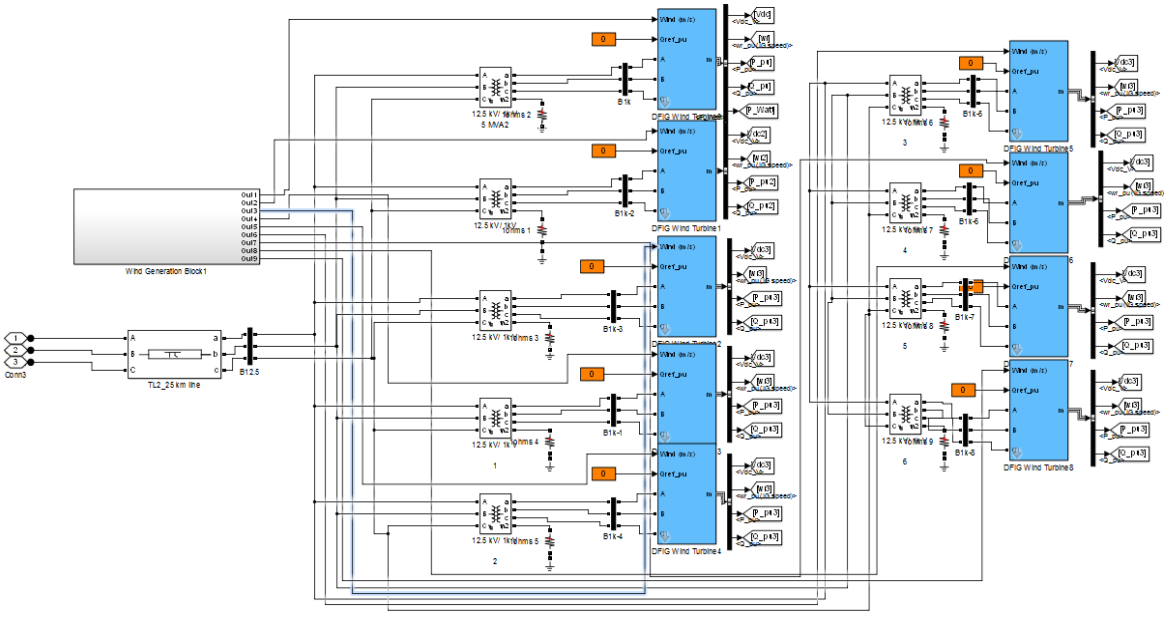

(b)

Figure 8. Simulink model of the wind farm: (a) general view of the model. (b) Fermeuse wind farm model.

Where r_s, r_r' are stator and rotor winding resistance of induction machine, L_{ls}, L_{lr}' are leakage inductance of stator and rotor winding, L_m is magnetizing inductance.

7. Results

Three different scenarios are considered: 1) at constant wind speed, 2) at variable wind speeds, and 3) when the

wind farm trips due to a fault and then reconnected to the grid.

Firstly, results of the system working under variable wind speeds are shown as below in **Figure 9** and **Figure 10**.

Secondly, the results of the system under constant wind speed at 15 m/s are as follows:

Comparing frequency and current, and so power, in these two scenarios, it is clear that variable wind speeds cause small fluctuations in the frequency and the current injected to the grid, meaning the grid is quite stiff.

Thirdly, the results in case of a fault happening at t = 3 s and the wind farm trips then it is reconnected to the grid at t = 5 s. **Figure 11** indicates measured and calculated values at receiving end of the line, at 69 KV bus.

Figure 12 depicts the voltage and current when fault happens measured from the sending end of the line, at 12.5 KV bus.

8. Conclusion

A Simulink model of the 27 MW wind farm, including 9 wind turbines with the power of 3 MW, transformers, transmission lines, utility grid, and measurement blocks, located in Fermeuse, NL, Canada, was presented in this paper and simulation results for three different scenarios were analyzed. This paper concludes that the developed model is able to represent the dynamics of the wind farm and its effect on the power system.

Table 3. Wind turbine specifications.

Rated power	3 MW
Rotor diameter	90 m
Nominal speed	16.1 rpm
Rotor speed range	9.9 - 18.4 rpm
Number of blades	3
Blade length	44 m
Gearbox ratio	1:109
Cut-in wind speed	4 m/s
Cut-out wind speed	25 m/s

Table 4. Induction generator parameters.

Type	DFIG
Nominal power	3 MW
Voltage	1000 V
Rated speed	1758 rpm
Number of poles	4
Total inertia constant	3.02 s
Friction coefficient	0.01
r_s , r_r'	2.35 mΩ, 1.67 mΩ
L_{ls} , L_{lr}'	0.151 H, 0.1379 H
L_m	2.47 H

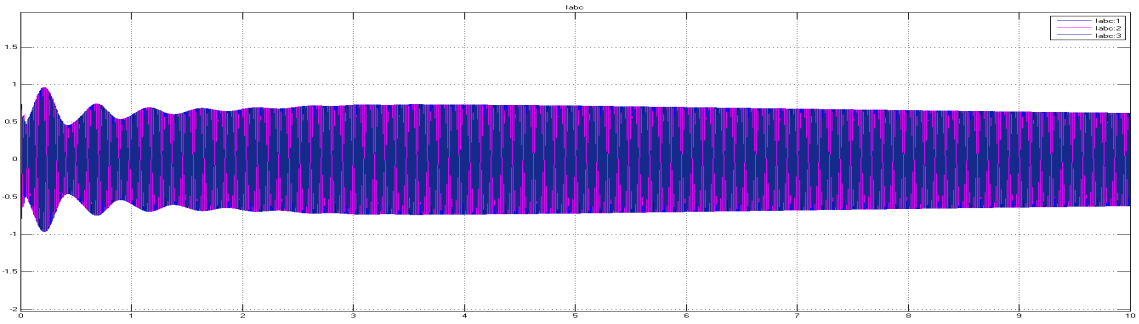

(a)

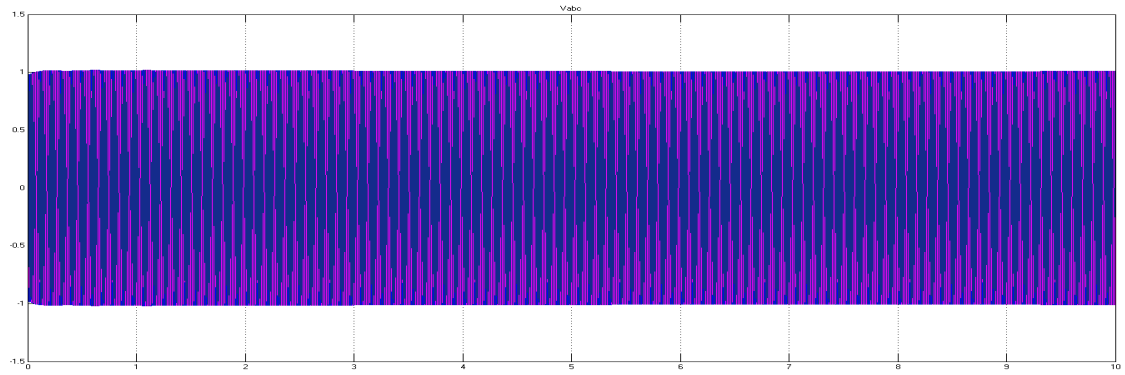

(b)

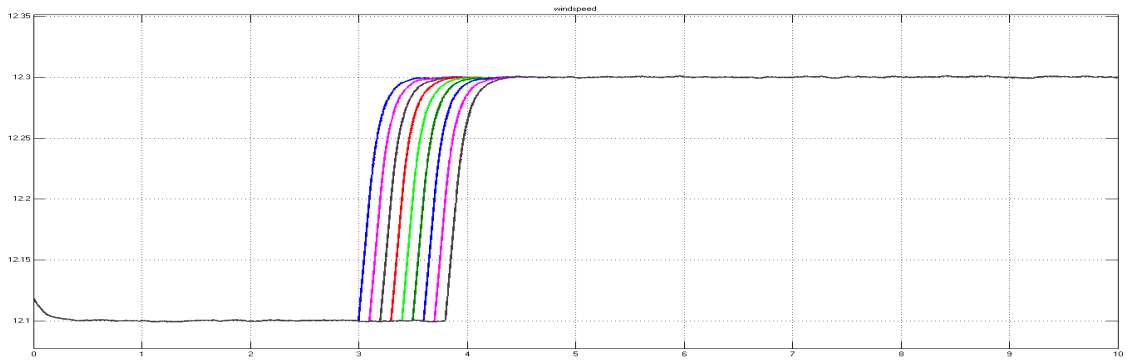

(c)

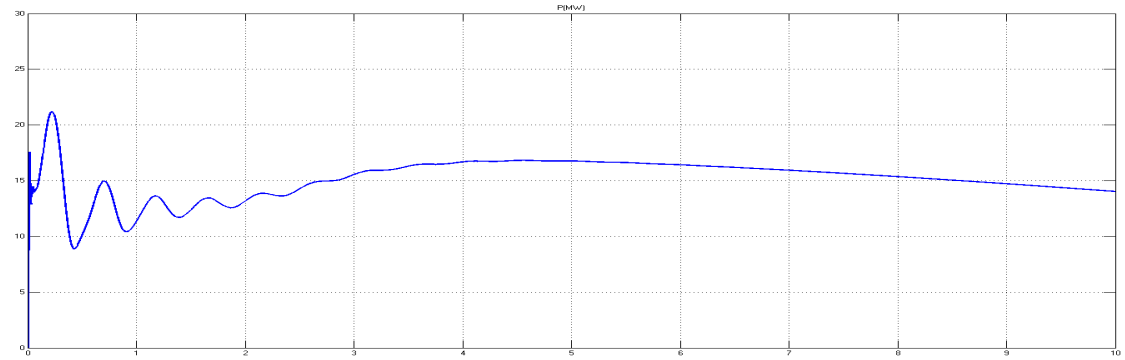

(d)

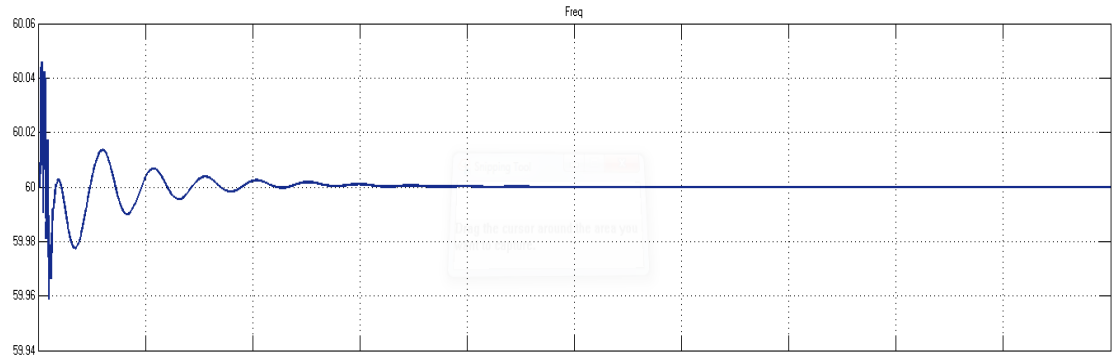

(e)

Figure 9. (a) to (d): Simulink model results for variable wind speeds. (a): Current; (b): Voltage; (c): Wind speed variations; (d): Power output; (e): Frequency.

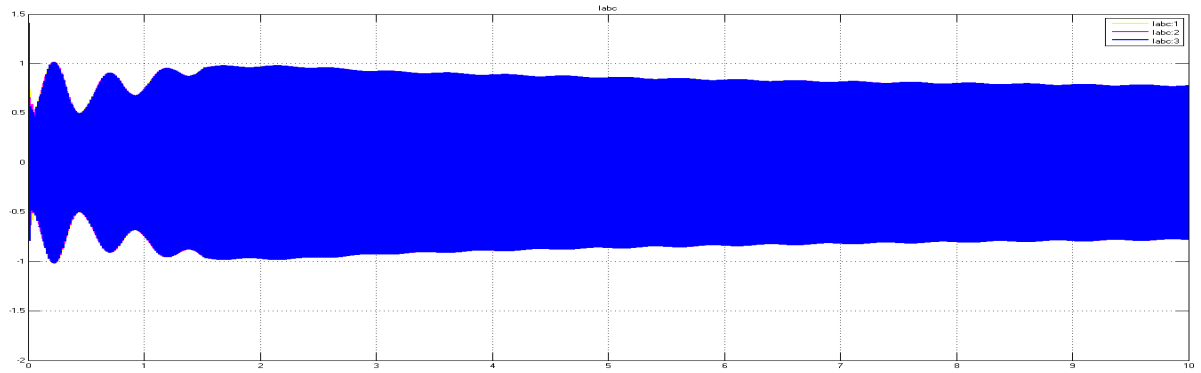

(a)

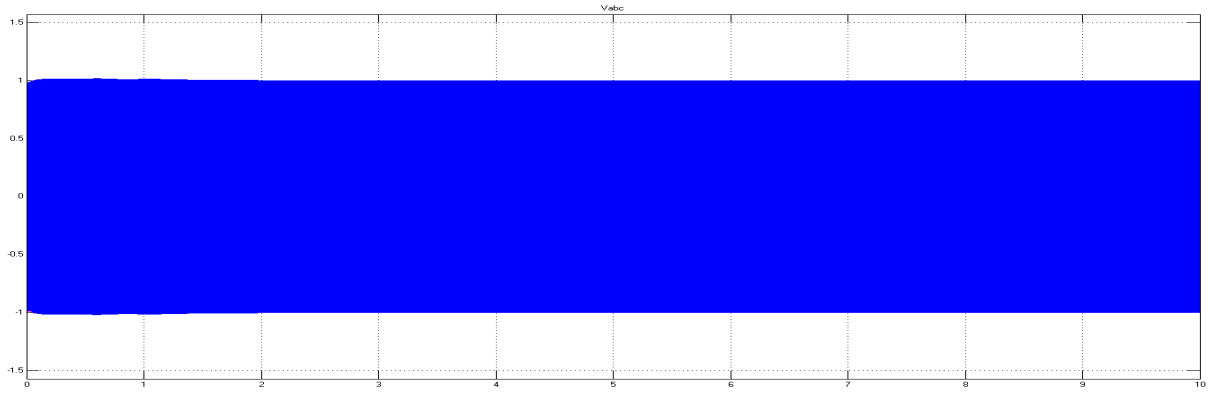

(b)

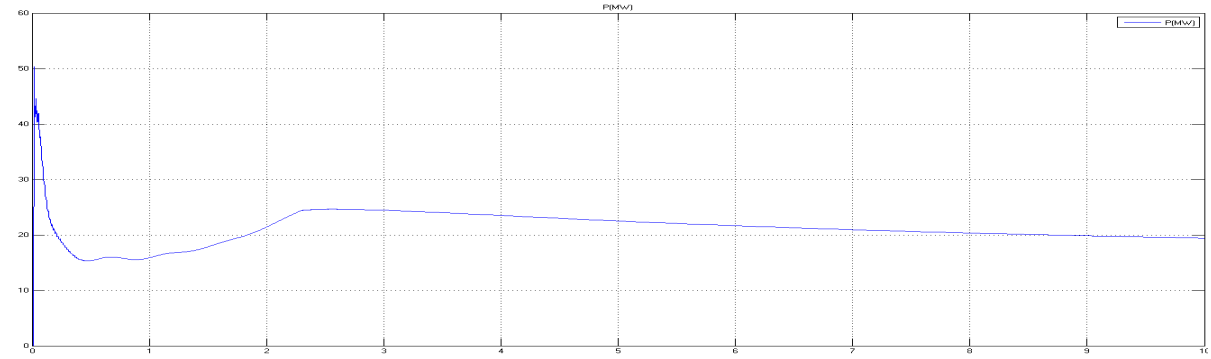

(c)

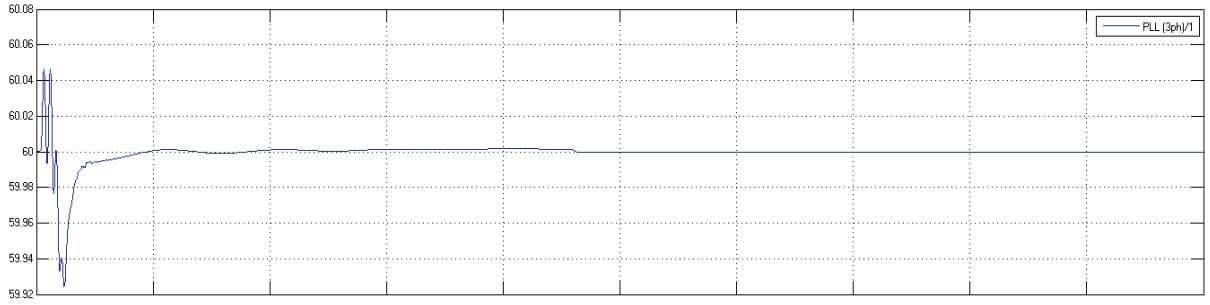

(d)

Figure 10. (a) to (d): Simulink model results for constant wind speed. (a): Current; (b): Voltage; (c): Power output; (d): Frequency.

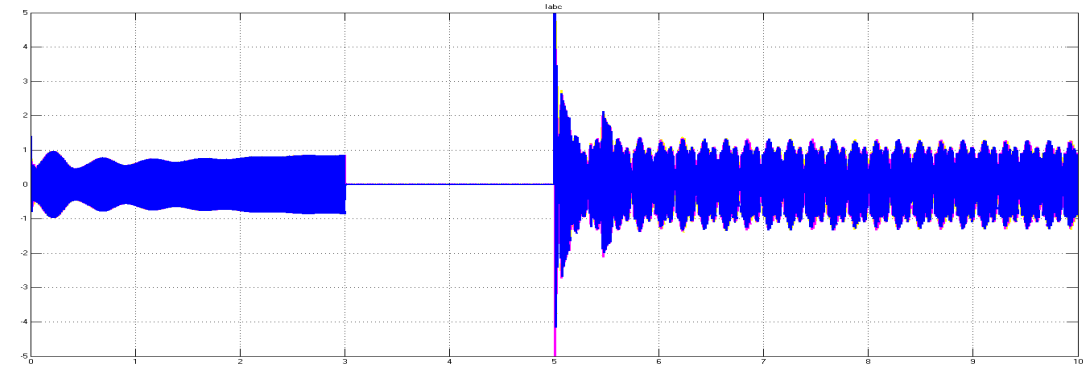

(a)

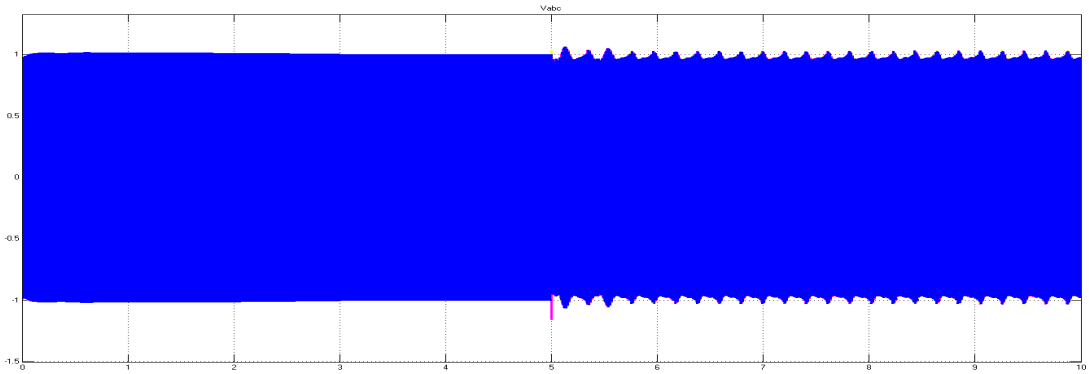

(b)

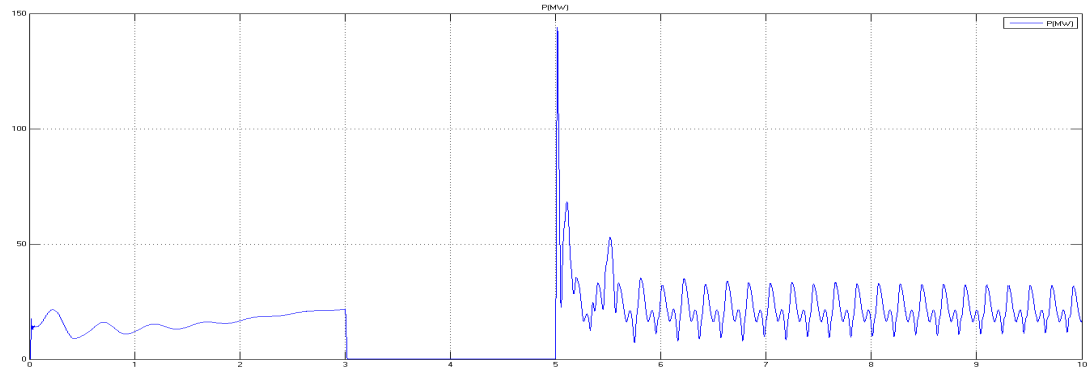

(c)

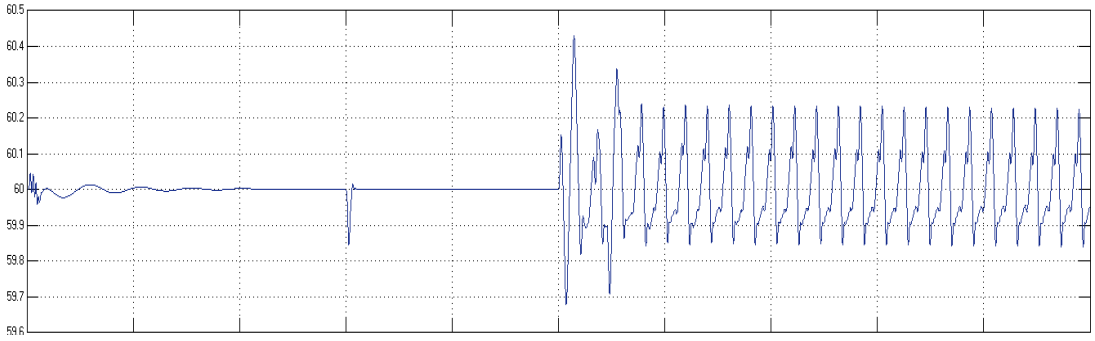

(d)

Figure 11. (a) to (d): Simulink results when fault occurs measured at receiving end. (a): Current; (b): Voltage; (c): Power output; (d): Frequency.

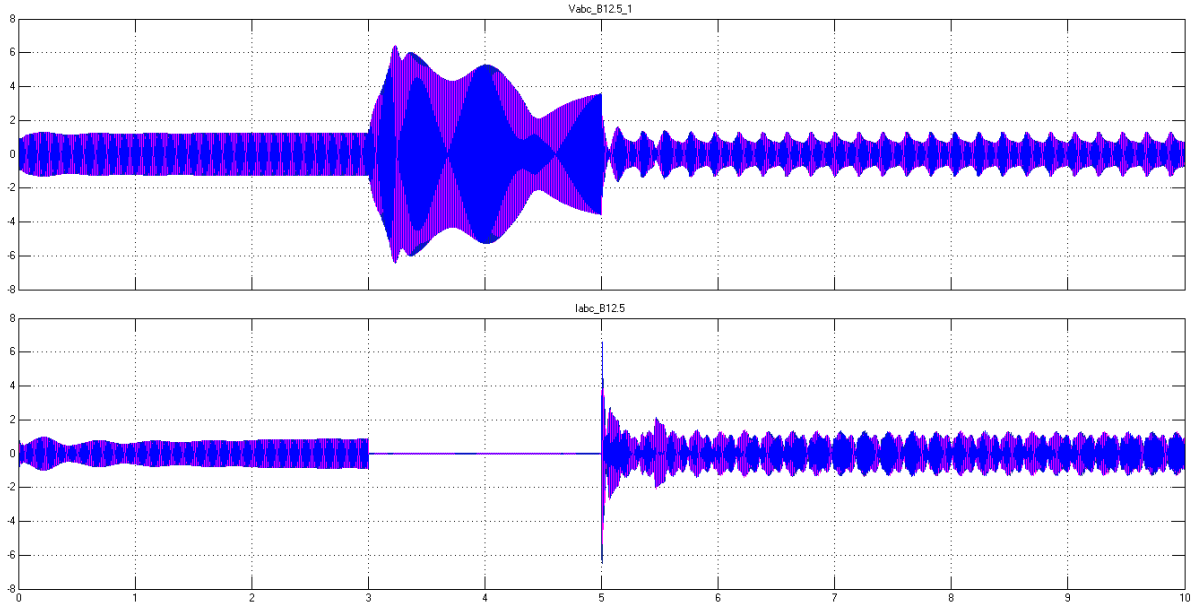

Figure 12. Simulink results when fault occurs measured at sending end.

References

[1] Blaabjerg, F., Teodorescu, R., Liserre, M. and Timbus, A.V. (2006) Overview of Control and Grid Synchronization for Distributed Power Generation Systems. *IEEE Transactions on Industrial Electronics*, **53**, 1398-1409. http://dx.doi.org/10.1109/TIE.2006.881997

[2] Abbey, C., Katiraei, F., Brothers, C., Dignard-Bailey, L. and Joos, G. (2006) Integration of Distributed Generation and Wind Energy in Canada. *IEEE Power Engineering Society General Meeting PES*'06 *Proceedings*, Montreal, 1-7. http://dx.doi.org/10.1109/pes.2006.1709430

[3] Expert Estimates, Based on Transmission Losses Published in Energy Statistics Handbook. A Joint Publication of Statistics Canada and Natural Resources. http://www.statcan.gc.ca/access_acces/alternative_alternatif.action?teng=57-601-x2012001-eng.pdf&tfra=57-601-x2012001-fra.pdf&l=eng&loc=57-601-x2012001-eng.pdf

[4] Schauder, C. and Mehta, H. (1993) Vector Analysis and Control of the Advanced Static VAR Compensators. *IEE Proceedings C*: *Generation*, *Transmission and Distribution*, **140**, 299-306.

[5] Iov, F., Hansen, A.D., Sørensen, P. and Blaabjerg, F. (2004) Wind Turbine Blockset in Matlab/Simulink. Aalborg University, Aalborg.

[6] Krause, P.C., Wasynczuk, O. and Sudhoff, S.D. and Pekarek, S. (2013) Analysis of Electric Machinery and Drive Systems, Vol. 75. John Wiley & Sons, Hoboken.

[7] http://www.mathworks.com/help/physmod/sps/examples/wind-farm-dfig-average-model.html

[8] Miller, N.W., Price, W.W. and Sanchez-Gasca, J.J.. (2003) Dynamic Modeling of GE 1.5 and 3.6 Wind Turbine-Generators. GE-Power Systems Energy Consulting.

[9] Iov, F., Hansen, A.D., Sørensen, P. and Cutulis, N.A. (2007) Mapping of Grid Faults and Grid Codes. Riso Report, Riso-R-1617(EN), Risø National Laboratory, Roskilde.

[10] Ackermann, T. (2005) Wind Power in Power Systems. John Wiley and Sons, Ltd., Hoboken, 58-110.

[11] http://www.vestas.com/Files/Filer/EN/Brochures/ProductbrochureV90_3_0_UK.pdf